Solar Energy Materials & Solar Cells 142 (2015) 54–59

Contents lists available at ScienceDirect

Solar Energy Materials & Solar Cells

journal homepage: www.elsevier.com/locate/solmat

Analysis of *n*-type IBC solar cells with diffused boron emitter locally blocked by implanted phosphorus

Ralph Müller*, Christian Reichel, Julian Schrof, Milan Padilla, Marisa Selinger, Ino Geisemeyer, Jan Benick, Martin Hermle

Fraunhofer Institute for Solar Energy Systems (ISE), Heidenhofstrasse 2, D-79110 Freiburg, Germany

ARTICLE INFO

Article history:
Received 31 March 2015
Received in revised form
22 May 2015
Accepted 28 May 2015
Available online 16 June 2015

Keywords:
Silicon solar cells
n-Type
Back-junction back-contact
Ion implantation
Reverse breakdown

ABSTRACT

Interdigitated back-contact (IBC) solar cells were fabricated with a process sequence combining local ion implantation of phosphorus and full area BBr_3 furnace diffusion resulting in conversion efficiencies of up to 22.4%. The highly doped emitter and BSF are in direct contact to each other (p^+n^+ junction) leading to a controlled junction breakdown at low reverse-bias voltages of around 5 V. The breakdown was located at the p^+n^+ junction and found to be homogeneously distributed over the whole cell area. This is not critical for module integration as the absolute temperature rise of a reverse-biased cell was determined to be less than 35 K. After reverse breakdown, the conversion efficiency degraded by 1–2% absolute due to additional recombination at the p^+n^+ junction. The cell performance could be fully recovered by a short annealing at 300 °C indicating that the Al_2O_3 passivation was altered by the reverse breakdown. This might be a fundamental issue for Al_2O_3 passivated IBC solar cells without gap between emitter and BSF, independent from the doping method.

1. Introduction

Interdigitated back-contact (IBC) solar cells have a very high efficiency potential [1–3] but typically come along with a complex fabrication process [4]. One promising approach to simplify the process sequence is the combination of ion implantation and furnace diffusion to form the differently doped regions [5] which is depicted in Fig. 1. This approach includes (i) local implantation of phosphorus to form the back surface field (BSF), (ii) subsequent BBr_3 furnace diffusion to form the rear emitter as well as the front floating emitter and (iii) a final etch to remove the borosilicate glass (BSG). One feature of this process sequence is the application of a boron diffusion to anneal the phosphorus implantation, i.e. activate the P atoms and drive them into the substrate. The annealing of phosphorus during boron diffusion has already been proven to work well by Kania et al., but in this study the authors do not reveal whether the P-implanted region was capped or not before entering the diffusion furnace [6]. For the process sequence shown in Fig. 1, a capping of the P-implanted region can be omitted as it was found that the strong phosphorus doping blocks the diffusion of boron very effectively [7]. Hence, only a very small amount of boron enters the P-implanted BSF region which consequently is compensated by a huge amount of phosphorus (see Fig. 1).

It has been published that this process sequence is suited for the fabrication of IBC solar cells [5]. As a consequence of the processing sequence, emitter and BSF regions are in direct contact to each other creating a sharp transition from p^+ to n^+ doping. Such p^+n^+ junctions are known as Zener diodes and are intentionally designed for a controlled breakdown at a certain reverse bias voltage. In IBC solar cells, such a controlled reverse breakdown can be in principle act as an integrated bypass diode [8–11]. On the other hand, an uncontrolled reverse breakdown can destroy solar cell and module by the thermal load if the power density and the resulting temperature is too high (the so called “hot spots”).

In this work we address the behavior of IBC solar cells fabricated with the process sequence shown in Fig. 1 under reverse bias with respect to performance stability and module integration. Therefore, solar cells with different doping profiles (p^+n^+ junction) and geometries (p^+n^+ junction meander length) were fabricated and characterized in forward and reverse operation. Additionally, lock-in and infrared thermography as well as electroluminescence imaging were used for a spatially-resolved investigation of the reverse breakdown and its impact on the solar cell performance.

* Corresponding author. Tel.: +49 761 4588x5921; fax: +49 761 4588x9250.
E-mail address: ralph.mueller@ise.fraunhofer.de (R. Müller).

http://dx.doi.org/10.1016/j.solmat.2015.05.046
0927-0248/

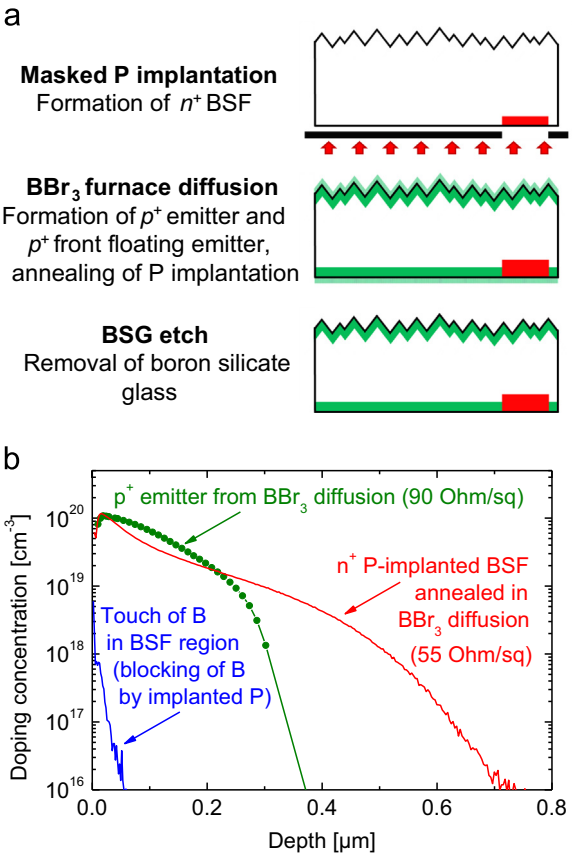

Fig. 1. Simplified process sequence for the fabrication of alternating *p*- and *n*-type regions for IBC solar cells featuring a synergistic combination of masked phosphorus implantation and BBr_3 furnace diffusion (a) [5] and doping profiles resulting from that process sequence measured by SIMS in the BSF region and ECV in the emitter (b) [5]. The experimental details can be found in Ref. [5] and correspond to the 1st batch of solar cells presented in this work.

2. Experimental

Solar cells were fabricated on 1 Ω cm *n*-type FZ silicon wafers with 200 μm thickness. The samples were textured on the front side with KOH forming random pyramids. Phosphorus was implanted locally on the back side (3×10^{15} cm^{-2}, 10 keV) to form the BSF. The ions were implanted through a 10 nm thick thermal oxide layer (surface protection, not relevant for the process itself) and masking was done by a photoresist, imitating a shadow mask which can also be applied for this step. Emitter and front floating emitter (FFE) [12] were realized by a BBr_3 furnace diffusion (890 °C, 1 h) followed by the removal of the borosilicate glass (BSG) in HF. The samples were passivated on both sides with 10 nm Al_2O_3 (PA-ALD) capped with 60 nm SiN_x (PECVD) on the front side and 100 nm SiO_x (PECVD) on the back side. Contact openings on the back side were etched in HF masked by a photoresist. Al was evaporated on the back side and wet-chemically structured also with a photoresist mask. A second batch of solar cells was fabricated similarly, but with a higher phosphorus implantation dose (1×10^{16} cm^{-2}) and an additional high-temperature step (30 min at 1000 °C in Ar atmosphere) after the BBr_3 diffusion and BSG etch. This drive-in served to push the dopants deeper into the substrate and to smooth the sharp transition from p^+ to n^+. Fig. 2 shows a cross-sectional sketch of the fabricated IBC solar cells.

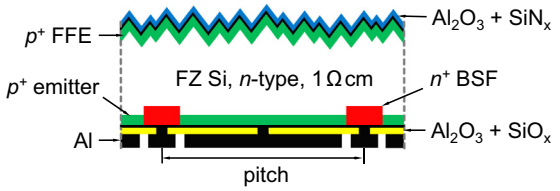

Fig. 2. Schematic of the IBC solar cell with BSF formed by local ion implantation of phosphorus and subsequent BBr_3 furnace diffusion [5]. In the first batch, the pitch is 2.2 mm with 1.9 mm emitter width and 0.3 mm BSF width. The dimensions were reduced in the second batch (0.9 mm pitch, 0.8 mm emitter width and 0.1 mm BSF width).

Table 1
Solar cell parameters of the best cells measured under standard testing conditions (AM1.5 G, 100 mW/cm^2, 25 °C). The aperture cell area is 4 cm^2. R_S was calculated from the comparison of Suns-V_{OC} and one-sun *IV* curve according to Ref. [13] and J_{02} was determined from fitting the dark *IV* curve with the two-diode model.

	V_{OC} [mV]	J_{SC} [mA/cm^2]	*FF* [%]	*PFF* [%]	R_S [Ω cm^2]	J_{02} [nA/cm^2]	η [%]
1st batch	674	40.0	80.6	83.4	0.52	12	21.7
2nd batch	672	41.0	81.5	82.8	0.23	17	22.4

3. Results and discussion

The solar cell parameters of the IBC cells investigated in this work are summarized in Table 1. The first batch was fabricated with a non-optimized phosphorus-implanted BSF and a BBr_3-diffused emitter. The second batch was processed similarly but with adapted doping profiles and cell geometry. An additional high-temperature step was included after the BBr_3 diffusion to drive the dopants deeper into the substrate and the pitch was reduced from 2.2 to 0.9 mm. Those two differences lead to an increase in J_{SC} and *FF* resulting in an absolute efficiency gain of 0.7%.

Together with the pitch, the BSF width was reduced as well (from 300 μm down to 100 μm). This leads to a weaker drop of the quantum efficiency above the BSF fingers, the so called “electrical shading” [14], and hence a significant gain in the short-circuit current density (J_{SC}). A further J_{SC} gain can be attributed to the reduced internal series resistance caused by lateral transport due to the lower pitch [15]. However, by lowering the pitch, the p^+n^+ junction meander length increases by a factor of 2.4 which raises the corresponding saturation current density (J_{02}). This leads to a slight drop of the pseudo fill factor (*PFF*), but the fill factor (*FF*) effectively increases due to the strong influence of the reduced series resistance (R_S).

3.1. Reverse breakdown

Fig. 3 shows the measured reverse current density for two IBC solar cells from the first and second batch under external reverse bias voltage. Additionally, an IBC cell with gap between emitter and BSF is shown [16]. The cell with gap has a large space charge region (SCR) all around the emitter which effectively inhibits the reverse current. A very low leakage current is flowing in reverse direction for external voltages down to −15 V. In contrast, the cells fabricated in this work without gap between emitter and BSF exhibit an early breakdown for low voltages in reverse direction. Therefore, the SCR is very small due to emitter and BSF being in direct contact and the resulting strong doping gradient from p^+ to n^+ [17]. With increasing reverse bias voltage, the SCR shrinks further and the reverse current increases. Cells from the second batch with drive-in of the dopants have deeper profiles and the peak concentrations are lower, so the transition from p^+ to n^+ is softer and the breakdown occurs at slightly higher reverse voltage.